Breast cancer-derived microparticles reduce cancer cell adhesion, an effect augmented by chemotherapy

Dvir Shechter[1], Michal Harel[2], Abhishek Mukherjee[3], Leonel M. Sagredo[4], David Loven[5], Elad Prinz[1], Shimrit Avraham[1], Veronique Orian-Rousseau[4], Tamar Geiger[2], Yuval Shaked [1,*], Haguy Wolfenson[3,*]

1. Department of Cell Biology and Cancer Science, Rappaport Faculty of Medicine, Technion – Israel Institute of Technology, Haifa, Israel.
2. Human Molecular Genetics and Biochemistry, Sackler Faculty of Medicine, Tel Aviv University, Tel Aviv, Israel.
3. Department of Genetics and Developmental Biology, Rappaport Faculty of Medicine, Technion – Israel Institute of Technology, Haifa, Israel.
4. Karlsruhe Institute of Technology, Institute of Biological and Chemical Systems – Functional Molecular Systems (IBCS-FMS), Karlsruhe, Germany.
5. Department of Oncology, Ha'Emek Medical Center, Afula, Israel.

***Co-corresponding authors**

Running title: Chemotherapy-induced pro-metastatic TMPs

Declaration: The authors declare no conflict of interest

Contact details:

Yuval Shaked	Haguy Wolfenson
Office: +972-4-829-5215	Office: +972-4-829-5239
email: yshaked@technion.ac.il	email: haguyw@technion.ac.il

ABSTRACT

Tumor-derived microparticles (TMPs), TMP, have been shown to support metastasis, in part by help forming the pre-metastatic niche. We and others have demonstrated that chemotherapy contributes to tumor cell aggressiveness via different mechanisms including TMP. However, the contribution of TMPs to cell adhesion properties as part of the metastatic cascade has not been fully demonstrated. Here we show that TMPs from highly metastatic cells or cells exposed to chemotherapy substantially reduce cell adhesion and disrupt actin filament structure therefore altering their biomechanical forces further implicating tumor cell dissemination as part of the metastatic cascade. These pro-metastatic effects are mediated in part by CD44 highly expressed in TMPs obtained from metastatic cells or cells exposed to chemotherapy when compared to cells with low metastatic potential. Consequently, pharmacological or genetic ablation of CD44 expressed by TMPs increases tumor cell adhesion and re-organizes actin filament structure. Increased CD44 expression in TMPs was also demonstrated in breast cancer patients after they were treated with paclitaxel chemotherapy. Overall, our study provides further insight into the role of TMPs in promoting metastasis, an effect which is augmented in response to chemotherapy.

Keywords: chemotherapy, breast cancer, adhesion, metastasis, CD44, extracellular vesicles.

INTRODUCTION

Although significant progress has been made in the last decades towards the development of novel anti-cancer therapies, most cancer types are still incurable, with metastasis being the main cause of death. In breast cancer, the most frequently diagnosed cancer in woman, approximately half a million cancer death due to metastasis is reported [1]. While the minority of breast cancer patients are diagnosed with stage IV advanced metastatic incurable disease, approximately 30% of all breast cancer women will develop metastasis within months to years since diagnosis [2]. Metastasis is a multi-step process that includes cancer cell dissemination from the primary tumor, intravasation to the blood or lymphatic system, survival in the circulation, extravasation to a target organ, and seeding and proliferation at a distal site [3, 4]. These effects require a tight regulation of the cellular machinery that supports tumor cell detachment from the primary tumor and their binding to the metastatic site.

Recently, microparticles, have emerged as having a potential significant role in tumor progression and metastasis. Microparticles belong to heterogeneous double layered membrane-coated particles exerted from cells, called extracellular vesicles (EVs) [5]. EVs encompass lipids, proteins, mRNA, non-coding RNA, and DNA. EVs have been studied mostly in the context of intercellular communication, whereby they transfer cargo between cells, including signaling proteins and RNA, as well as stimulate cells by membrane binding [5, 6]. There are three main family members of EVs: apoptotic bodies (1000-4000nm in diameter), microparticles (100-1000nm in diameter) and exosomes (20-100nm in diameter) [5, 7]. EVs have been shown to affect cancer progression in various ways. For example, at remote secondary sites, the EVs are taken up by organ-derived cells, thereby preparing the microenvironment for future tumor cell seeding. These effects are associated with integrins expressed by EVs which direct them to specific organs [8]. In melanoma, EVs derived from tumors contribute to the mobilization of myeloid cells to the pre-metastatic site and support metastasis [9]. Such pro-metastatic niche formation has been recently reported to be enhanced in response to chemotherapy [10]. Perhaps the most significant effect of EVs on cancer progression occurs at the primary tumor site, where EVs transfer oncogenic proteins such as EGFRvIII between glioblastoma cells, therefore supporting tumorigenesis [11]. In addition, the transfer of CD44/CD44v6 expressed by EVs support tumor initiation and progression [12]. Similarly, CD44-expressing EVs also contribute to metastasis by remodeling the ECM within the primary tumor, supporting tumor cell invasion [13].

When focusing on microparticles, it has been shown that tumor-derived microparticles (TMPs) obtained from multi-drug resistant breast cancer cells, support immune evasion by polarizing macrophages into inactive state. This process contributes to the colonization of breast cancer cells at distant sites [14]. In another study, TMPs were shown to selectively transfer p-glycoprotein to breast cancer cells, supporting their multidrug resistance capacity and therefore contribute to tumor growth [15]. We have recently

demonstrated that breast cancer cells exposed to chemotherapy shed an increased number of TMPs expressing osteopontin. These TMPs support the mobilization and tumor homing of pro-angiogenic bone marrow derived cells (BMDCs), ultimately enhancing tumor growth and metastasis [16]. However, little is known about the effect of TMPs on the biomechanical pro-metastatic effects of cells within the primary tumor site that support their dissemination, and the contribution of chemotherapy to this process.

Here we show that TMPs from highly metastatic tumor cells or cells exposed to chemotherapy enhance the metastatic characteristics of low-metastatic recipient cells within the primary tumor microenvironment. These effects include changes in focal adhesions, actin cytoskeleton rearrangement, and alterations in transmission of biomechanical forces, all driven by EV expressing CD44, and leading to the dissemination of recipient cells from the primary tumor and ultimately increased metastasis. Thus, this study describes a biomechanical mechanism that drives the metastatic switch in chemotherapy-treated tumors.

Materials and Methods

Cell culture

MDA-MB-231 human breast carcinoma cells, 4T1 murine breast carcinoma cells, and HEK293T human embryonic kidney cells were purchased from the American Type Culture Collection (ATCC). The LM2-4 cell line, a lung metastatic variant of the MDA-MB-231 cell line, was kindly provided by Prof. Robert Kerbel (Sunnybrook Health Sciences Centre, Toronto, Ontario, Canada). 67NR, is a low metastatic variant of the 4T1 cell line, was kindly provided by Prof. Jonathan Sleeman (Medical Faculty Mannheim, Centre for Biomedicine and Medical Technology Mannheim (CBTM), University of Heidelberg, Mannheim 68167, Germany). In some cases, cells were fluorescently tagged with green fluorescent protein (GFP). All cells were used within 6 months of resuscitation. Human cell lines were cultured in RPMI 1640 (Sigma-Aldrich) and murine cell lines in Dulbecco's Modified Eagle's Medium (Sigma-Aldrich). In all cases, medium was supplemented with 5% fetal bovine serum (FBS), 1% l-glutamine, 1% sodium pyruvate, and 1% streptomycin, penicillin and neomycin in solution (10 mg/ml, Biological Industries, Israel). Cells were tested routinely to be mycoplasma-free. Human cell lines were tested to be authentic or they have been used within 6 months from resuscitation.

Extraction and quantification of TMP

The extraction and quantification of TMPs were carried out as previously demonstrated and validated [15-18]. Briefly, cells were grown to 80% confluency, at which point medium was replaced with serum free (SF) medium or SF supplemented with 200 nM paclitaxel (PTX), as previously described [16]. After 48

hours, conditioned medium (CM) was collected and centrifuged at 4000*g* for 20 min at RT to remove floating cells and apoptotic bodies. Supernatants were collected and centrifuged at 20,000*g* for 1 hour at 4°C. The TMP-containing pellet was resuspended in phosphate buffered saline (PBS) and stored at −80°C until further use. It should be noted that the dosage of 200nM PTX for a duration of 48 hours in serum-free conditions did not result in cell death, excluding the possibility that samples were contaminated with apoptotic bodies, as previously described [16].

TMP quantification was performed using flow cytometry by calculating the ratio between 7.35 µm counting beads (Calbiochem) and the number of events collected in the TMP gate (approximately 0.6–0.9 µm) as previously described [16, 19]. Additional information is found in Supplemental Online Materials.

Quantification and measurement of TMPs by Nanosight NS300 (Malvern,UK) was performed as previously described [20]. Additional information is found in Supplemental Online Materials.

Modified Boyden chamber assay

The invasion properties of MDA-MB-231 cells pre-exposed to different TMP conditions were evaluated in Matrigel coated Boyden chambers as previously described [21]. Additional information is found in Supplemental Online Materials.

Cell spreading assay

TMPs were pre-exposed to 1µg/ml IgG or anti-CD44 (BioXcell, West Lebanon, NH, USA) for 1 hour followed by extensive washing in which a volume of 100 times PBS was used. The TMPs were then added to MDA-231-MB GFP+ cultures, and incubated for 24 hours. Subsequently, the cells were trypsinized and re-plated on fibronectin coated glass plates. Time lapse movies were generated from images acquired every 5 minutes for a total of 4 hours using an ImageXpress Micro Confocal system (Molecular Devices, San Jose, CA). The percentage of cells spreading over fibronectin was analyzed using FIJI, as previously described [22].

Cell viability AlamarBlue™ assay

The metabolic indicator dye AlamarBlue™ (Serotec Ltd., Oxford, UK) was used to determine cell viability, as previously described [23]. Additional information is found in Supplemental Online Materials.

Pillar fabrication

Pillar fabrication was performed as previously described [22, 24]. Briefly, PDMS (Sylgard 184, Dow Corning; 10:1 base to curing agent ratio) was poured over silicon molds with wells that were 1.3 µm deep, 0.5 µm wide, and spaced 1 µm apart (center-to-center distance). The molds were then flipped-over onto

glass-bottom dishes (no. 0 glass coverslip, Cellvis), which were then placed at 60°C for 12 h to cure the PDMS. The molds were peeled off from the plates while immersed in pure ethanol, which was then replaced by PBS. The pillars were coated with fibronectin (10 μg/ml, 1 hr, 37°C). To measure cellular forces on the fibronectin-coated pillars, serum-starved MDA-MB-231 cells were cultured for 24 hours in the presence of 100,000 TMPs obtained from untreated or PTX-treated MDA-MB-231 cells, or from untreated or PTX-treated LM2-4 cells. The cells were then spread on the pillar arrays and imaged at 37°C using a Leica DMIRE2 microscope, 100x 1.4 NA oil objective, and a CCD camera (QImaging Retiga EXi). Analyses of pillar movements was performed with ImageJ (National Institutes of Health) using the Nano Tracking plugin as previously described [22]. Pillar displacement curves were generated using Matlab. Analyses of pillar releases by the cells was performed on the pillar displacement curves using the 'findpeaks' function in Matlab. All peaks identified were categorized into bins ranging from 1 to 25 nm, and the number of releases per second were calculated for each of these bins. For each condition >30 pillars from >3 cells were analyzed.

CD44 short hairpin RNA

Several different shRNA sequences specific to human CD44 or a scrambled control sequence were cloned into the GIPZ Lentiviral Human shRNA plasmid (Horizon discovery, Lafayette, CO), as previously described [25]. Subconfluent LM2-4 cells were transfected with shRNA plasmids using lipofectamine reagent (Thermo Fisher Scientific, MA) according to the manufacturer's instructions. Forty-eight hours post-transfection, cells were incubated in growth medium containing puromycin (1 μl/ml) for the selection of stable transfectants. After 3 weeks of selection, the protein level of CD44 was evaluated by flow cytometry using appropriate controls. Two independent CD44-depleted clones generated from the pooled cells were selected for this study.

Western blot

Paxillin and phospho-paxillin analysis was performed as follows. MDA-MB-231 cells were pre-exposed to 100,000 TMPs for 24 hours, and then seeded on a fibronectin (20μg/ml) coated plate overnight. Subsequently, the cells were lysed in Hepes 50 mM PH-7.5, EDTA 4 mM, Triton 1%, 0.5 mg/ml Na3VO4, 4.5 mg/ml Na2P2O7 and lysates were subjected to SDS-PAGE. Proteins were electro-transferred to nitrocellulose membranes, which were then probed with polyclonal rabbit anti-paxillin (1:1000; Cell Signaling, Catalog number 2542), anti-phospho-paxillin (1:1000; Cell Signaling, catalog number 2541), or anti-GAPDH (1:5000, Santa Cruz Biotechnology, Inc., Catalog number sc-25778). GAPDH was used as loading controls. All experiments were performed in triplicate.

Extracellular vesicle proteomics

Extracellular vesicle proteomics were assessed and analyzed in accordance with the previously described method [26]. Briefly, TMPs were isolated by multiple centrifugations of conditioned media from MDA-MB-231 and LM2-4 cells cultured in serum free media in the presence or absence of PTX as described above. Pellets were immediately resuspended in 200µl of lysis buffer (6 M urea, 2 M thiourea in 0.1 M Tris pH 7.6). Protein concentration was calculated based on Bradford assay, and 10µg of each sample was used for the analysis. The proteins were reduced using 1 mM DTT and alkylated using 5 mM iodoacetamide, followed by overnight in-solution trypsin/LysC digestion. The peptides were acidified with 0.1% TFA and purified on C18 stageTips [27]. A total of three biological replicates were prepared for each system, some of which were analyzed with two technical replicates, and were later combined into a single data point.

Resulting peptides were analyzed by LC-MS/MS on the EASY-nLC1000 UHPLC system (Thermo Scientific) coupled to the Q-Exactive Plus mass spectrometer (Thermo Scientific). The peptides were separated using a gradient of 140 min (technical replicate I) or 240 min (technical replicate II) of water-acetonitrile on a 50 cm EASY-spray column. Data were acquired using a top-10 method in a data-dependent mode. Resolution values were 70,000 and 17,500 in the MS and MS/MS scans, respectively.

MS raw files were processed using MaxQuant version 1.5.6.9 [28] and the Andromeda search engine [29]. MS/MS spectra were searched against the human uniprot database on a forward and decoy database with 1% false discovery rate for both the protein and the peptide levels. The 'match between runs' option was enabled to transfer identifications between runs. The Label-free algorithm was used for protein quantification. Technical replicates were averaged into a single biological replicate during the MaxQuant data processing. The proteinGroups output was further analyzed using the Perseus software [30]. Label-free quantification (LFQ) intensity values [31] were log2 transformed. Each comparison (MDA-MB-231 vs. MDA-MB-231 PTX or MDA-MB-231 vs. LM2-4) was processed separately, following data filtration that kept only proteins that were quantified in at least two of the three replicates in at least one of the sample groups. Student t-test was performed with permutation-based FDR correction with a cutoff of 0.1 and S0 correction of 0.2 [32]. Enrichment analysis was done using Fisher exact test with FDR cutoff of 0.02. Principal component analysis (PCA) was performed following data imputation, by replacing the missing values with values that form a normal distribution with a downshift of 1.6 standard deviations and width of 0.4 of the original data distribution.

Ex vivo pulmonary metastasis assay

Ex-vivo pulmonary metastasis assay (PuMA) was performed as previously described [33, 34]. Additional information is found in Supplemental Online Materials.

Blood samples from cancer patients

The study was approved by the hospital' Ethic Committee (Ha'Emek medical center), and written informed consent was obtained from all involved patients, in compliance with the Helsinki declaration for human studies. Patients with localized breast carcinoma were treated by neoadjuvant chemotherapy (before tumor removal) consisting of adriamycin and cyclophosphamide followed by paclitaxel chemotherapy at the HaEmek Medical Center, Afula, Israel. Blood was collected in 5 ml sodium citrate (3.2%) tubes before the first cycle of paclitaxel chemotherapy and 24 hours post-treatment (n=15). Plasma was obtained by centrifugation at 1000 g for 10 min at RT. Subsequently, platelet-poor plasma (PPP) was extracted by plasma centrifugation at 3000g for 5 min at RT as previously described [35]. This procedure eliminates most of the platelets (<10,000 per µl). To ensure purified PPP, another centrifugation (3000g for 5 min) was performed on separated PPP at RT. Subsequently PPP was stored at -80oC. Thawed PPP was centrifuged at 20,000g for 1 hour, and the pellet was resuspended in PBS. Anti-MUC-1 antibody and anti-CD44 antibody were added according to manufacturer's instructions, and subsequently analyzed by flow cytometry as described below. Fluorescence-minus-one control (FMO) was used to determine nonspecific binding of antibodies as previously described [36].

Immunostaining and imaging

Serum-starved cells were cultured for 24 hours in the presence of 100,000 TMPs obtained from untreated or PTX-treated cells as indicated in the text. In some experiments, TMPs were cultured with cells for 24 hours in serum-free medium in the presence of Annexin V (0.5µg/ml) or anti-CD44 antibodies (1µg/ml). Cells were rigorously washed in PBS (100 fold volume), and then seeded on fibronectin-coated plates (20 µg/ml fibronectin, Biological Industries, Israel). After 4 hours, cells were fixed using 4% paraformaldehyde (PFA), and immunostained with a primary anti-vinculin antibody (1:100, Sigma-Aldrich), and Cy2-conjugated secondary antibody. Actin was stained with Alexa 488 conjugated phalloidin (1:100, Invitrogen). Images were acquired with LSM 700 Zeiss confocal microscope (Zeiss).

Statistical Analysis

Data are presented as mean ± standard error (SE). All in vitro studies were performed at least in three biological replicates. The in vivo studies were performed twice. Statistically significant differences were assessed by one-way ANOVA, followed by Tukey post-hoc test (when comparing between more than two groups) using GraphPad Prism 6 software (La Jolla, CA, USA). When applicable, estimate of variance was

performed and statistical significance comparing only two sets of data was determined by two-tailed Student's t-test. Significance was set at values of $p<0.05$, and designated as follows: *,$p < 0.05$; **$p < 0.01$; ***$p < 0.001$.

RESULTS

TMPs from highly metastatic or chemotherapy-treated tumor cells induce tumor cell invasion

To study the effect of TMPs on the metastatic potential and the adhesion properties of tumor cells, we compared TMPs from MDA-MB-231 cells with their highly metastatic variant, LM2-4 cells [37]. TMPs were extracted from the medium and quantified by flow cytometry and NanoSight. While the number of TMPs extracted from highly metastatic cells or from cells exposed to chemotherapy was higher than control cells, as previously published [10, 16], their size was not significantly different as evaluated by NanoSight (Figure S1). Based on their size, we ruled out the possibility that some of the TMPs detected are apoptotic bodies, as also previously published [16].

We next postulated that TMPs from highly metastatic cells or from cells exposed to chemotherapy could augment the metastatic potential of low-metastatic cells. To this end, TMPs were extracted from MDA-MB-231 and LM2-4 cells which had been treated with PTX or vehicle control. Subsequently, these TMPs were cultured with low-metastatic MDA-MB-231 cells for 24 hours and further analyzed for invasion properties using the Boyden chamber assay. TMPs from PTX-treated MDA-MB-231 cells enhanced the invasive properties of MDA-MB-231 cells in comparison to control cultures including TMPs from non-treated MDA-MB-231 cells or serum-free conditions. Furthermore, MDA-MB-231 cells cultured with TMPs from control or PTX-treated LM2-4 cells exhibited the highest invasive ability (Figure 1A-B). Notably, TMPs from PTX-treated cells displayed induced invasion properties regardless of the metastatic potential of the tumor cells, implicating a potent effect of chemotherapy on TMP-induced cell invasion. Similar results were observed when using 4T1 highly metastatic cells and their low metastatic 67NR cells (Figure 1C-D). Of note, TMPs had no effect on proliferation (Figure S2). Taken together, these results suggest that TMPs affect tumor cell invasion properties.

TMPs from highly metastatic or chemotherapy-treated tumor cells inhibit tumor cell seeding

We next sought to test if TMPs affect the seeding of low metastatic cells in distant tissues. We therefore performed an ex vivo pulmonary metastasis assay (PuMA), which primarily evaluates the seeding potential of tumor cells in the lungs [34]. GFP-expressing MDA-MB-231 cells pre-cultured for 24 hours with TMPs from vehicle- or PTX-treated MDA-MB-231 or LM2-4 cells, were injected through the tail vein of naïve mice to perform the PuMA. Interestingly, fluorescence microscopy and flow cytometry analyses revealed that tumor cell seeding in the lungs was reduced when the MDA-MB-231 cells were pre-cultured

with TMPs from PTX-treated MDA-MB-231 cells or with TMPs from vehicle- or PTX-treated LM2-4 cells (Figure 2A-C). Taking into account the short time interval between cell injection and animal sacrifice, these results suggest that the TMPs lowered the cells' adhesive ability. Indeed, cells exposed to TMPs from PTX-treated MDA-MB-231 cells or to TMPs from vehicle- or PTX-treated LM2-4 cells spread to a much lower extent when seeded on fibronectin-coated plates compared to control conditions (Figure 2D-E), a property that directly relates to the inability of forming strong cell-matrix adhesions [22]. Once again, TMPs from PTX-treated cells displayed similar reduced tumor cell adhesion properties regardless of the metastatic potential of the tumor cells, therefore suggesting a strong effect of chemotherapy on TMPs which hinder cell adhesion.

TMPs from highly metastatic or chemotherapy-treated tumor cells inhibit cellular adhesion and destruct actin filaments

Metastatic cells acquire the ability to detach from the primary tumor by inhibiting adhesion molecules and rearranging the actin cytoskeleton to promote the migratory properties [38]. To study the effect of TMPs on the cell adhesion, MDA-MB-231 cells were cultured for 24 hours in the presence of TMPs from vehicle- or PTX-treated MDA-MB-231 or LM2-4 cells, and then seeded on fibronectin-coated plates. After 4 hours, cells were fixed and stained with an anti-vinculin antibody and fluorescently-labeled phalloidin to label focal adhesions by vinculin expression and the actin cytoskeleton, respectively. A decreased number of adhesions in cells cultured with TMPs from PTX-treated MDA-MB-231 cells or with TMPs from vehicle- or PTX-treated LM2-4 cells were observed based on vinculin expression (Figure 3A-B). In addition, cell area was reduced in the presence of TMPs from all groups in comparison to control cells cultured in the absence of TMPs (Figure 3C). Lastly, cells cultured with TMPs from PTX-treated MDA-MB-231 cells or with TMPs from vehicle- or PTX-treated LM2-4 cells seem to demonstrate less organized and elongated actin stress fibers such as those observed in control cells (Figure 3D). Thus, TMPs support metastatic cell characteristics by means of downregulating formation of mature adhesion plaques and less organized actin cytoskeleton.

TMPs support metastatic cell biomechanical forces

Since there is a reciprocal regulation between adhesions and their associated force-producing actin cytoskeleton [39], we sought to determine which of these structures was affected by TMPs, thereby affecting the other. When MDA-MB-231 cells were cultured with TMPs from LM2-4 or from PTX-exposed cells, they pulled on the matrix at a similar pace compared to control cells. However, they could not maintain their hold, leading to repeated pull/release cycles that occurred at a higher rate in comparison to control cells (Figure 4A-C). Since defects in cytoskeletal assembly lead to changes in the rate of force

application, whereas defects in adhesions lead to their breakage [22], we concluded that exposure to TMPs from LM2-4 or from PTX-exposed cells directly affects cell adhesion properties, rendering the adhesions too weak to withstand cytoskeletal forces and preventing the formation of stress fibers. Furthermore, Western blot analysis of cell lysates revealed significantly lower adhesion-associated paxillin signaling in cells cultured with TMPs from PTX-treated MDA-MB-231 cells or with TMPs from vehicle- or PTX-treated LM2-4 cells (Figure 4D-E), suggesting that cell adhesion is reduced in cells exposed to TMPs from PTX-treated cells or highly metastatic cells. Overall, our results demonstrate that TMPs from PTX-treated low metastatic cells or from highly metastatic cells (regardless of chemotherapy treatment) disrupt cell adhesion, which is consistent with cell dissemination and increased ability to invade.

Proteomic analysis of TMPs

We next undertook a proteomic approach to identify factors within TMPs that affect cell adhesion, when the major focus was placed on adhesion related proteins. To this end, TMPs were isolated from MDA-MB-231 and LM2-4 cells (untreated or treated with PTX) and processed for high-resolution mass-spectrometry-based proteomic analysis. Overall, 5209 proteins were identified, with control MDA-MB-231 TMPs exhibiting the lowest number of proteins (Table S1). Principal component analysis further reflected the large variation between control MDA-MB-231 TMPs and all other TMP groups (Figure 5A). We then performed two comparisons: in the first, we compared between the proteomes of TMPs derived from control and PTX-treated MDA-MB-231 cells; in the second, we compared between the proteomes of TMPs derived from control MDA-MB-231 cells and untreated LM2-4 cells. Over 300 significantly altered proteins were detected in each comparison, calculated by Student's t-test, FDR 0.1, and S0=0.2, as previously described [32] (Figure 5B-C). When specifically focusing on adhesion membrane proteins whose levels were changed, 15 proteins were common to both comparisons (Figure 5D), 14 of which were higher in MDA-MB-231 control TMPs, including Lysyl Oxidase Like 2 (LOXL2)**,** Laminin Subunit Gamma 1 and Gamma 2 (LAMC1 and LAMC2), and Tenascin C (TNC). Interestingly, out of the 15 cell adhesion proteins common to both comparisons, only one, CD44, was significantly increased in TMPs from PTX-treated MDA-MB-231 or untreated LM2-4 cells (Figure 5D). Its intensity in these TMPs was over 2-fold higher than in TMPs derived from control MDA-MB-231 cells (Figure 5E). Altogether, these results suggest that CD44, probably among other proteins that are differentially expressed between the various TMP groups, is a possible co-effector that can potentially account for the disruption of cell adhesion induced by TMPs.

CD44-expressing TMPs affect cell adhesion and support tumor cell metastatic properties

CD44 is a glycoprotein known to participate in cell adhesion and migration [40, 41]. Therefore, increased levels of CD44 in TMPs may explain the TMP-induced effects on the adhesive and invasive properties of

tumor cells. To test this, TMPs derived from untreated or PTX-treated MDA-MB-231 or LM2-4 cells were incubated with CD44 blocking antibodies or IgG control antibodies for 24 hours. Excess antibodies were removed by rigorous washing when adding a 100-fold volume of PBS to the sample followed by centrifugation to obtain TMPs. Subsequently, the TMPs were added to MDA-MB-231 cultures, and invasive and adhesive properties were assessed. Pre-treating TMPs with anti-CD44 antibodies restored the invasive properties of TMP-exposed tumor cells to control levels (Figure S3A-B). Similar results were obtained when TMPs from 4T1 cells were pre-treated with anti-CD44 antibodies and subsequently cultured with NR67 (low metastatic) cells (Figure S3C-D).

Next, TMPs pre-treated with anti-CD44 were added to MDA-MB-231 cultures, and the number of focal adhesions assessed by vinculin, cell area, efficiency of cell spreading, and the phenotype of actin stress fibers were evaluated. Blocking CD44 on TMPs from highly metastatic cells or from cells exposed to chemotherapy restored the conditions found in control MDA-MB-231 cells. Specifically, CD44 inhibition on TMPs increased focal adhesion plaques assessed by vinculin, cell area, and percentage of cell spreading (Figure 6A-D). Notably, cell size reduction noticed in MDA-MB-231 cells exposed to TMPs from PTX-treated or LM2-4 cells seems to be in line with cell spreading demonstrated in Figure 2D. Furthermore, TMPs in which CD44 was inhibited resulted in rearrangement of actin stress fibers, mimicking those found in control serum-free conditions (Figure 6E). Similar results were obtained when TMPs from highly metastatic cells were knocked down for CD44 and subsequently were added to MDA-MB-231 cultures, where clones 1 and 2 demonstrated increased number of focal adhesion plaques assessed by vinculin and better organization of actin filaments when compared to scrambled control cells (Figure S4). Taken together, these results further indicate that CD44-expressing TMPs contribute to the inhibition of cell adhesion and cytoskeleton re-arrangement, and thus enhancing the metastatic properties of tumor cells.

TMPs expressing CD44 were increased in breast cancer patients treated with chemotherapy

To further investigate the possibility that TMPs expressing CD44 found in breast cancer patients following chemotherapy, we collected plasma samples from 15 breast cancer patients at baseline or 24 hours after paclitaxel chemotherapy administration. We used MUC-1 as an epithelial breast carcinogenic marker, known also to be expressed on TMPs [16]. The number of MUC-1+/CD44+ TMPs detected in plasma samples from 12 out of 15 breast cancer patients post-chemotherapy was 3-4 fold higher than those at baseline (Figure 7A-B). Taken together, the data suggest that chemotherapy induces CD44 expression on TMPs and as a result may contribute to tumor cell aggressiveness.

DISCUSSION

Metastasis is the main cause of death in cancer patients, and is still a major obstacle for success of therapy. Treatment protocols involve chemotherapy, radiation, surgery, or a combination thereof. These protocols have shown clinical benefit, yet resistance is common and recurrence following chemotherapy is usually more aggressive [42, 43]. In previous studies we and others have demonstrated that the host-mediated response to chemotherapy provides a suitable yet partial explanation for therapy-induced metastasis and tumor recurrence, as described in preclinical and clinical studies [42, 43]. Here, we explore one possible mechanism by which a communication between different tumor cell populations within the primary tumor mass contributes to metastatic aggressiveness, especially in response to chemotherapy. Specifically, we demonstrate that TMPs originating from highly metastatic or chemotherapy-exposed tumor cells mediate a paracrine effect that alters cell adhesion and rearranges the actin cytoskeleton, therefore promoting early stage metastatic properties in recipient low metastatic tumor cells.

We demonstrate that the pro-metastatic effects of TMPs are associated with the expression of CD44, a non-oncogenic protein. EVs expressing CD44 have been shown to promote tumor cell aggressiveness and metastasis mainly by contributing to the pre-metastatic niche [12, 44]. Here we found that TMPs expressing CD44 contribute to metastatic tumor cell characteristics in part by disrupting the actin cytoskeleton filament structure, inhibiting focal adhesion plaques and cell spreading, reducing contractility, and downregulating adhesion-related signaling measured by phospho-paxillin. While these effects clearly contribute to the understanding of the extracellular function of CD44, studies need further investigation regarding the intracellular domain of CD44. Specifically, it has been shown that the intracellular domain of CD44 recruits actin binding complexes such as ezrin, radixin, moesin (ERM), and ankyrin [45]. These complexes are associated with intracellular signaling via Ras-MAPK, Wnt and PI3K [12], and thus can contribute to the metastatic characteristics of tumor cells by other mechanisms. Notably, while our study focused on specific adhesion molecules, based on the proteomic analysis it is plausible that other molecules expressed by TMPs may affect cell adhesion properties, including specific extracellular matrix associated enzymes. Thus, additional studies in this direction will provide further insights into the overall effects of TMPs on tumor cell metastatic characteristics.

Elevated CD44 expression levels were also found in TMPs from breast cancer patients treated with PTX. When analyzing their plasma samples, we focused on MUC1+ EVs that are known to originate from tumor cells in various malignancies, suggesting they are TMPs [16, 46]. The percentage of TMPs expressing CD44 was increased in plasma samples from breast cancer patients following chemotherapy when compared to baseline levels. However, it should be noted that TMPs in the plasma may vary in quantity over time due to high clearance rate [47]. Thus, it will be of interest to study the dynamic changes in TMPs expressing MUC1+CD44 in cancer patients treated with chemotherapy. Nevertheless, our results further suggest that

the expression of CD44 is elevated in TMPs following chemotherapy in patients, in agreement with our findings in mice.

In summary, we describe a mechanism whereby CD44 expressing TMPs affect tumor cell metastatic characteristics by altering cell adhesion properties. This effect is augmented in response to chemotherapy, leading to enhanced metastasis. Indeed, in breast cancer patients it has been demonstrated that chemotherapy may elicit increased tumor microenvironment of metastasis (TMEM). These TMEMs promote the dissemination of tumor cells from the primary tumor site [48]. It is plausible that combining chemotherapy with agents that explicitly inhibit CD44 on TMPs may inhibit chemotherapy-induced tumor cell dissemination to potentially form metastasis, and therefore can serve as a strategy to inhibit possible risks of chemotherapy-induced metastasis in breast cancer.

Author contributions

Conception and design: DS, TG, HW, and YS.

Acquisition of data: DS, MH, AM, LMS, DL, EP and SA.

Analysis and interpretation of data: DS, MH, LMS, VOR, TG, HW, and YS.

Writing, review, and/or revision of the manuscript: DS, MH, VOR, TG, HW, and YS.

Study supervision: HW and YS.

Acknowledgments

This study was supported by grants primarily from the European Research Council (771112) given to YS, from the Israel Science Foundation (1738/17) given to HW, and from the Rappaport Institute funds given to YS and HW. HW is an incumbent of the David and Inez Myers Career Advancement Chair in Life Sciences. The authors declare that they have no conflict of interest.

REFERENCES

1. Jemal, A.; Bray, F.; Center, M. M.; Ferlay, J.; Ward, E.; Forman, D., Global cancer statistics. *CA Cancer J Clin* **2011,** *61* (2), 69-90.

2. O'Shaughnessy, J., Extending survival with chemotherapy in metastatic breast cancer. *Oncologist* **2005,** *10 Suppl 3*, 20-9.

3. Sahai, E., Illuminating the metastatic process. *Nature reviews. Cancer* **2007,** *7* (10), 737-49.

4. Welch, D. R.; Hurst, D. R., Defining the Hallmarks of Metastasis. *Cancer Res* **2019,** *79* (12), 3011-3027.

5. van Niel, G.; D'Angelo, G.; Raposo, G., Shedding light on the cell biology of extracellular vesicles. *Nat Rev Mol Cell Biol* **2018,** *19* (4), 213-228.

6. Raposo, G.; Stahl, P. D., Extracellular vesicles: a new communication paradigm? *Nat Rev Mol Cell Biol* **2019,** *20* (9), 509-510.

7. Lee, T. H.; D'Asti, E.; Magnus, N.; Al-Nedawi, K.; Meehan, B.; Rak, J., Microvesicles as mediators of intercellular communication in cancer--the emerging science of cellular 'debris'. *Semin Immunopathol* **2011,** *33* (5), 455-67.

8. Hoshino, A.; Costa-Silva, B.; Shen, T. L.; Rodrigues, G.; Hashimoto, A.; Tesic Mark, M.; Molina, H.; Kohsaka, S.; Di Giannatale, A.; Ceder, S.; Singh, S.; Williams, C.; Soplop, N.; Uryu, K.; Pharmer, L.; King, T.; Bojmar, L.; Davies, A. E.; Ararso, Y.; Zhang, T.; Zhang, H.; Hernandez, J.; Weiss, J. M.; Dumont-Cole, V. D.; Kramer, K.; Wexler, L. H.; Narendran, A.; Schwartz, G. K.; Healey, J. H.; Sandstrom, P.; Labori, K. J.; Kure, E. H.; Grandgenett, P. M.; Hollingsworth, M. A.; de Sousa, M.; Kaur, S.; Jain, M.; Mallya, K.; Batra, S. K.; Jarnagin, W. R.; Brady, M. S.; Fodstad, O.; Muller, V.; Pantel, K.; Minn, A. J.; Bissell, M. J.; Garcia, B. A.; Kang, Y.; Rajasekhar, V. K.; Ghajar, C. M.; Matei, I.; Peinado, H.; Bromberg, J.; Lyden, D., Tumour exosome integrins determine organotropic metastasis. *Nature* **2015,** *527* (7578), 329-35.

9. Peinado, H.; Aleckovic, M.; Lavotshkin, S.; Matei, I.; Costa-Silva, B.; Moreno-Bueno, G.; Hergueta-Redondo, M.; Williams, C.; Garcia-Santos, G.; Ghajar, C.; Nitadori-Hoshino, A.; Hoffman, C.; Badal, K.; Garcia, B. A.; Callahan, M. K.; Yuan, J.; Martins, V. R.; Skog, J.; Kaplan, R. N.; Brady, M. S.; Wolchok, J. D.; Chapman, P. B.; Kang, Y.; Bromberg, J.; Lyden, D., Melanoma exosomes educate bone marrow progenitor cells toward a pro-metastatic phenotype through MET. *Nat.Med.* **2012,** *18* (6), 883-891.

10. Keklikoglou, I.; Cianciaruso, C.; Guc, E.; Squadrito, M. L.; Spring, L. M.; Tazzyman, S.; Lambein, L.; Poissonnier, A.; Ferraro, G. B.; Baer, C.; Cassara, A.; Guichard, A.; Iruela-Arispe, M. L.; Lewis, C. E.; Coussens, L. M.; Bardia, A.; Jain, R. K.; Pollard, J. W.; De Palma, M., Chemotherapy elicits pro-metastatic extracellular vesicles in breast cancer models. *Nature cell biology* **2019,** *21* (2), 190-202.

11. Al-Nedawi, K.; Meehan, B.; Micallef, J.; Lhotak, V.; May, L.; Guha, A.; Rak, J., Intercellular transfer of the oncogenic receptor EGFRvIII by microvesicles derived from tumour cells. *Nature cell biology* **2008,** *10* (5), 619-24.

12. Wang, Z.; Zhao, K.; Hackert, T.; Zoller, M., CD44/CD44v6 a Reliable Companion in Cancer-Initiating Cell Maintenance and Tumor Progression. *Front Cell Dev Biol* **2018,** *6*, 97.

13. Nakamura, K.; Sawada, K.; Kinose, Y.; Yoshimura, A.; Toda, A.; Nakatsuka, E.; Hashimoto, K.; Mabuchi, S.; Morishige, K. I.; Kurachi, H.; Lengyel, E.; Kimura, T., Exosomes Promote Ovarian Cancer Cell Invasion through Transfer of CD44 to Peritoneal Mesothelial Cells. *Mol Cancer Res* **2017,** *15* (1), 78-92.

14. Jaiswal, R.; Johnson, M. S.; Pokharel, D.; Krishnan, S. R.; Bebawy, M., Microparticles shed from multidrug resistant breast cancer cells provide a parallel survival pathway through immune evasion. *BMC Cancer* **2017,** *17* (1), 104.

15. Jaiswal, R.; Luk, F.; Dalla, P. V.; Grau, G. E.; Bebawy, M., Breast cancer-derived microparticles display tissue selectivity in the transfer of resistance proteins to cells. *PloS one* **2013,** *8* (4), e61515.

16. Fremder, E.; Munster, M.; Aharon, A.; Miller, V.; Gingis-Velitski, S.; Voloshin, T.; Alishekevitz, D.; Bril, R.; Scherer, S. J.; Loven, D.; Brenner, B.; Shaked, Y., Tumor-derived microparticles induce bone marrow-derived cell mobilization and tumor homing: a process regulated by osteopontin. *International journal of cancer. Journal international du cancer* **2014,** *135* (2), 270-81.

17. Issman, L.; Brenner, B.; Talmon, Y.; Aharon, A., Cryogenic transmission electron microscopy nanostructural study of shed microparticles. *PloS one* **2013,** *8* (12), e83680.

18. Ma, R.; Ji, T.; Chen, D.; Dong, W.; Zhang, H.; Yin, X.; Ma, J.; Liang, X.; Zhang, Y.; Shen, G.; Qin, X.; Huang, B., Tumor cell-derived microparticles polarize M2 tumor-associated macrophages for tumor progression. *Oncoimmunology* **2016,** *5* (4), e1118599.

19. Timaner, M.; Kotsofruk, R.; Raviv, Z.; Magidey, K.; Shechter, D.; Kan, T.; Nevelsky, A.; Daniel, S.; de Vries, E. G. E.; Zhang, T.; Kaidar-Person, O.; Kerbel, R. S.; Shaked, Y., Microparticles from tumors exposed to radiation promote immune evasion in part by PD-L1. *Oncogene* **2019**.

20. Bachurski, D.; Schuldner, M.; Nguyen, P. H.; Malz, A.; Reiners, K. S.; Grenzi, P. C.; Babatz, F.; Schauss, A. C.; Hansen, H. P.; Hallek, M.; Pogge von Strandmann, E., Extracellular vesicle measurements with nanoparticle tracking analysis - An accuracy and repeatability comparison between NanoSight NS300 and ZetaView. *J Extracell Vesicles* **2019,** *8* (1), 1596016.

21. Gingis-Velitski, S.; Loven, D.; Benayoun, L.; Munster, M.; Bril, R.; Voloshin, T.; Alishekevitz, D.; Bertolini, F.; Shaked, Y., Host response to short-term, single-agent chemotherapy induces matrix metalloproteinase-9 expression and accelerates metastasis in mice. *Cancer Res* **2011,** *71* (22), 6986-96.

22. Wolfenson, H.; Meacci, G.; Liu, S.; Stachowiak, M. R.; Iskratsch, T.; Ghassemi, S.; Roca-Cusachs, P.; O'Shaughnessy, B.; Hone, J.; Sheetz, M. P., Tropomyosin controls sarcomere-like contractions for rigidity sensing and suppressing growth on soft matrices. *Nature cell biology* **2016,** *18* (1), 33-42.

23. Voloshin, T.; Gingis-Velitski, S.; Bril, R.; Benayoun, L.; Munster, M.; Milsom, C.; Man, S.; Kerbel, R. S.; Shaked, Y., G-CSF supplementation with chemotherapy can promote revascularization and subsequent tumor regrowth: prevention by a CXCR4 antagonist. *Blood* **2011,** *118* (12), 3426-3435.

24. Ghassemi, S.; Meacci, G.; Liu, S.; Gondarenko, A. A.; Mathur, A.; Roca-Cusachs, P.; Sheetz, M. P.; Hone, J., Cells test substrate rigidity by local contractions on submicrometer pillars. *Proc Natl Acad Sci U S A* **2012,** *109* (14), 5328-33.

25. Schmitt, M.; Metzger, M.; Gradl, D.; Davidson, G.; Orian-Rousseau, V., CD44 functions in Wnt signaling by regulating LRP6 localization and activation. *Cell Death Differ* **2015,** *22* (4), 677-89.

26. Harel, M.; Oren-Giladi, P.; Kaidar-Person, O.; Shaked, Y.; Geiger, T., Proteomics of microparticles with SILAC Quantification (PROMIS-Quan): a novel proteomic method for plasma biomarker quantification. *Molecular & cellular proteomics : MCP* **2015,** *14* (4), 1127-36.

27. Rappsilber, J.; Mann, M.; Ishihama, Y., Protocol for micro-purification, enrichment, pre-fractionation and storage of peptides for proteomics using StageTips. *Nat Protoc* **2007,** *2* (8), 1896-906.

28. Tyanova, S.; Temu, T.; Cox, J., The MaxQuant computational platform for mass spectrometry-based shotgun proteomics. *Nat Protoc* **2016,** *11* (12), 2301-2319.

29. Cox, J.; Neuhauser, N.; Michalski, A.; Scheltema, R. A.; Olsen, J. V.; Mann, M., Andromeda: a peptide search engine integrated into the MaxQuant environment. *J Proteome Res* **2011,** *10* (4), 1794-805.

30. Tyanova, S.; Cox, J., Perseus: A Bioinformatics Platform for Integrative Analysis of Proteomics Data in Cancer Research. *Methods Mol Biol* **2018,** *1711*, 133-148.

31. Cox, J.; Hein, M. Y.; Luber, C. A.; Paron, I.; Nagaraj, N.; Mann, M., Accurate proteome-wide label-free quantification by delayed normalization and maximal peptide ratio extraction, termed MaxLFQ. *Molecular & cellular proteomics : MCP* **2014,** *13* (9), 2513-26.

32. Tusher, V. G.; Tibshirani, R.; Chu, G., Significance analysis of microarrays applied to the ionizing radiation response. *Proc Natl Acad Sci U S A* **2001,** *98* (9), 5116-21.

33. Mendoza, A.; Hong, S. H.; Osborne, T.; Khan, M. A.; Campbell, K.; Briggs, J.; Eleswarapu, A.; Buquo, L.; Ren, L.; Hewitt, S. M.; Dakir el, H.; Garfield, S.; Walker, R.; Merlino, G.; Green, J. E.; Hunter, K. W.; Wakefield, L. M.; Khanna, C., Modeling metastasis biology and therapy in real time in the mouse lung. *J Clin Invest* **2010,** *120* (8), 2979-88.

34. Rachman-Tzemah, C.; Zaffryar-Eilot, S.; Grossman, M.; Ribero, D.; Timaner, M.; Maki, J. M.; Myllyharju, J.; Bertolini, F.; Hershkovitz, D.; Sagi, I.; Hasson, P.; Shaked, Y., Blocking Surgically Induced Lysyl Oxidase Activity Reduces the Risk of Lung Metastases. *Cell reports* **2017,** *19* (4), 774-784.

35. Sultan, A., Five-minute preparation of platelet-poor plasma for routine coagulation testing. *East Mediterr Health J* **2010,** *16* (2), 233-6.

36. Hulspas, R.; O'Gorman, M. R.; Wood, B. L.; Gratama, J. W.; Sutherland, D. R., Considerations for the control of background fluorescence in clinical flow cytometry. *Cytometry B Clin Cytom* **2009,** *76* (6), 355-64.

37. Munoz, R.; Man, S.; Shaked, Y.; Lee, C.; Wong, J.; Francia, G.; Kerbel, R. S., Highly efficacious non-toxic treatment for advanced metastatic breast cancer using combination UFT-cyclophosphamide metronomic chemotherapy. *Cancer Res* **2006,** *66*, 3386-3391.

38. Bachir, A. I.; Horwitz, A. R.; Nelson, W. J.; Bianchini, J. M., Actin-Based Adhesion Modules Mediate Cell Interactions with the Extracellular Matrix and Neighboring Cells. *Cold Spring Harb Perspect Biol* **2017,** *9* (7).

39. Livne, A.; Geiger, B., The inner workings of stress fibers - from contractile machinery to focal adhesions and back. *J Cell Sci* **2016,** *129* (7), 1293-304.

40. Xu, H.; Tian, Y.; Yuan, X.; Wu, H.; Liu, Q.; Pestell, R. G.; Wu, K., The role of CD44 in epithelial-mesenchymal transition and cancer development. *Onco Targets Ther* **2015,** *8*, 3783-92.

41. Orian-Rousseau, V., CD44, a therapeutic target for metastasising tumours. *Eur J Cancer* **2010,** *46* (7), 1271-7.

42. Shaked, Y., Balancing efficacy of and host immune responses to cancer therapy: the yin and yang effects. *Nat Rev Clin Oncol* **2016,** *13* (10), 611-26.

43. Shaked, Y., The pro-tumorigenic host response to cancer therapies. *Nature reviews. Cancer* **2019**.

44. McFarlane, S.; McFarlane, C.; Montgomery, N.; Hill, A.; Waugh, D. J., CD44-mediated activation of alpha5beta1-integrin, cortactin and paxillin signaling underpins adhesion of basal-like breast cancer cells to endothelium and fibronectin-enriched matrices. *Oncotarget* **2015,** *6* (34), 36762-73.

45. Ponta, H.; Sherman, L.; Herrlich, P. A., CD44: from adhesion molecules to signalling regulators. *Nat Rev Mol Cell Biol* **2003,** *4* (1), 33-45.

46. Zwicker, J. I.; Liebman, H. A.; Neuberg, D.; Lacroix, R.; Bauer, K. A.; Furie, B. C.; Furie, B., Tumor-derived tissue factor-bearing microparticles are associated with venous thromboembolic events in malignancy. *Clinical cancer research : an official journal of the American Association for Cancer Research* **2009,** *15* (22), 6830-40.

47. Matsumoto, A.; Takahashi, Y.; Chang, H. Y.; Wu, Y. W.; Yamamoto, A.; Ishihama, Y.; Takakura, Y., Blood concentrations of small extracellular vesicles are determined by a balance between abundant secretion and rapid clearance. *J Extracell Vesicles* **2020,** *9* (1), 1696517.

48. Karagiannis, G. S.; Pastoriza, J. M.; Wang, Y.; Harney, A. S.; Entenberg, D.; Pignatelli, J.; Sharma, V. P.; Xue, E. A.; Cheng, E.; D'Alfonso, T. M.; Jones, J. G.; Anampa, J.; Rohan, T. E.; Sparano, J. A.; Condeelis, J. S.; Oktay, M. H., Neoadjuvant chemotherapy induces breast cancer metastasis through a TMEM-mediated mechanism. *Sci Transl Med* **2017,** *9* (397).

FIGURE LEGENDS

Figure 1: TMPs affect cell invasion. (A-D) TMPs were collected from MDA-MB-231 or LM2-4 cells (A-B) or from 67NR or 4T1 cells (C-D) which had been cultured for 48 hours in the presence of 200 nM paclitaxel (PTX) or vehicle control. The TMPs from the different groups were cultured with MDA-MB-231 cells for 24 hours. As a control, MDA-MB-231 cells were cultured alone in serum-free medium (SF). Cells from each treatment group were then seeded into Boyden chambers to assess cell invasion properties. Representative images of invading cells are shown in (A, C). Scale bar 200 µm. Quantifications of invading cells are shown in (B, D) (n= 5 repeats and 7 images/repeat). *differences compared to MDA-231-MB control or 67NR control group - ***, $p<0.001$, as assessed by One Way ANOVA followed by Tukey post-hoc test.

Figure 2: TMPs alter tumor cell seeding. (A-C) GFP-positive MDA-MB-231 cells were cultured for 24 hours in SF or in the presence of TMPs collected from MDA-MB-231 or LM2-4 cells which had been cultured for 48 hours in the presence of 200 nM paclitaxel (PTX) or vehicle control. GFP-positive cells were then intravenously injected to mice for an ex vivo pulmonary metastasis assay (PuMA) as described in Materials and Methods. Lung sections (n= 4 mice/group) were imaged (A) and the number of metastatic foci were counted (B). Scale bar 0.2 cm. White arrows point at metastatic foci. The percentage of metastatic cells in the lungs was also assessed by flow cytometry after the lung sections underwent single cell suspension (C). (D-E) Cells (treated as in A-C) were seeded onto fibronectin-coated plates. Cell spreading was then immediately assessed by time-lapse microscopy. Representative images are shown in (D). Scale bar 20 µm. Cell cytoplasmic membrane and nucleus are drawn in black line. Percentage of spread cells is shown in (E). n=3 repeats/group with the assessment of ~100 cells/repeat. *differences compared to MDA-231-MB control group,*, $p<0.05$, as assessed by One Way ANOVA followed by Tukey post-hoc test.

Figure 3: TMPs affect focal adhesions and cell structure. TMPs were collected from MDA-MB-231 or LM2-4 cells which had been cultured for 48 hours in the presence of 200 nM paclitaxel (PTX) or vehicle control. The TMPs from the different groups were then cultured with MDA-MB-231 cells for 24 hours. As a control, MDA-MB-231 cells were cultured alone in serum-free medium (SF). (A-C) The cells from each treatment group were seeded on fibronectin-coated plates. After 4 hours, cells were immunostained with anti-vinculin antibodies (green) and analyzed by confocal microscopy to assess focal adhesion plaques. Representative images (left panel) with X16 zoom micrographs (right panel) are shown. Scale bar 20 µm. White arrows point at focal adhesion plaques (A). The number of focal adhesions per cell was quantified (B). Cell area was calculated (C). n= 10 fields/group. (D) Fixed cells were stained with phalloidin (green) to assess actin filament structure. Representative images are shown (right panel) with x16 zoom micrographs

(left panel). Scale bar 20 µm. n=5 fields/group. *differences compared to MDA-231-MB control group,*, $p<0.05$; ***, $p<0.001$ as assessed by One Way ANOVA followed by Tukey post-hoc test.

Figure 4: TMPs affect cell biomechnical forces and inhibit focal adhesion signaling. (A-C) TMPs were collected from MDA-MB-231 or LM2-4 cells which had been cultured for 48 hours in the presence of 200 nM paclitaxel (PTX) or vehicle control. The TMPs from the different groups were then cultured with MDA-MB-231 cells for 24 hours. The cells were then evaluated using pillar assay as described in Materials and Methods. (A) Left: Example of a cell spreading on an array of 0.5 µm diameter fibronectin-coated pillars that are used to measure cellular forces through cell-matrix adhesions by live-cell imaging of pillar displacements (see illustration on the right). (B) Typical pillar displacement curves show that control cells (two left panels) were able to generate pillar displacements of up to 80-90 nm, but cells exposed to TMPs from LM cells or from MDA cells exposed to PTX failed to do so due to frequent releases of the pillars (note that pillar releases are also observed in the control cases, but there are recovery phases that lead to high overall displacements which are lacking in the three right curves). (C) Histograms presenting the average number of pillar releases per second binned according to the size of the release (all breaks up to 100 nm were measured; the histogram displayed here shows those that are up to 25 nm for clarity). Each of the control conditions, MDA-MB-231 or MDA-MB-231 exposed to TMPs from MDA-MB-231 cells (MDA-MB-231-Cont) was significantly different than the conditions in which the cells were exposed to TMPs from LM2-4 cells or from cells exposed to PTX ($\alpha<0.01$; Kolmogorov-Smirnov test), indicating more frequent releases at high forces due to adhesion breakage. n=8-10 repeats/group. (D-E) Cells treated as above were seeded on fibronectin-coated plates. Cells were harvested and lysed 24 hours later. The levels of phospho-paxillin (P-Pax) and total-paxillin (T-Pax) were analyzed by Western blot. GAPDH was used as a loading control (D). Densitometry analysis of the Western blot when the ratio between P-Pax overT-Pax was calculated and presented as fold change, for three biological repeats (E). n=3 repeats/group. *differences compared to MDA-231-MB control group,*, $p<0.05$, as assessed by One Way ANOVA followed by Tukey post-hoc test.

Figure 5: Proteomic analysis of TMPs identifies CD44 as a potential adhesion regulator common to both highly metastatic and PTX-treated cells. TMPs, collected from MDA-MB-231 or LM2-4 cells which had been cultured for 48 hours in the presence of 200nM paclitaxel (PTX) or vehicle control, were analyzed by mass spectrometry. (A) Principal component analysis shows clear separation between MDA-MB-231 control and the rest of the samples. (B-C) Heatmap (left) and volcano plot (right) for the comparison between control and PTX-treated MDA-MB-231 (B) or control MDA-MB-231 and LM2-4 (C). Overall, the levels of 202 and 167 proteins were higher in MDA-MB-231 PTX or LM2-4 TMPs (positive T-test difference

values), respectively, whereas the levels of 103 and 136 proteins were higher in the MDA-MD-231 control TMPs in both comparisons (negative T-test difference values). T-test differences are in log2 scale. In blue- "cell adhesion" proteins (GOBP category). Altogether, the level of CD44 was significantly higher in both PTX-exposed cells and highly metastatic cells. (D) T-test difference (log2 scale) of the "cell adhesion" proteins that were common to both comparisons. (E) CD44 LFQ-intensity in MDA-MB-231 and LM2-4 cells with and without PTX. The proteomic analysis was performed when n=3 repeats / group.

Figure 6: TMPs expressing CD44 affect tumor cell adhesion and structure. TMPs were collected from MDA-MB-231 or LM2-4 cells which had been cultured for 48 hours in the presence of 200 nM paclitaxel (PTX) or vehicle control. The TMPs from the different groups were incubated with anti-CD44 (5µg/ml) or control IgG for 24 hours, and subsequently rigorously washed. TMPs were then added to MDA-MB-231 cultures for 24 hours. As a control, MDA-MB-231 cells were cultured alone in serum-free medium (SF). (A-C) The cells were seeded on fibronectin-coated plates. After 4 hours, cells were fixed and immunostained with anti-vinculin antibodies (green) and analyzed by confocal microscopy to assess focal adhesion plaques. Representative images are shown (left panel) with x16 zoom micrographs (right panel). Scale bar 20 µm. White arrows point at focal adhesion plaques (A). The number of focal adhesions per cell was quantified (B). Cell area was calculated (C). n= 10-11 fields / group. (D) Cell spreading was analyzed with time-lapse microscopy. The percentages of spread cells per field are shown. n=5 repeats/group. (E) Fixed cells were stained with phalloidin (green) to assess actin filament structure. Representative images are shown (right panel) and x16 zoom micrographs (left panel). Scale bar 20 µm. n=5 fields/group. *differences compared to MDA-231-MB control group, *, $p<0.05$; **, $p<0.01$; ***, $p<0.001$, #differences between IgG and anti-CD44 of the same group, as assessed by One Way ANOVA followed by Tukey post-hoc test.

Figure 7: Elevated CD44 expression in peripheral TMPs from breast cancer patients who underwent chemotherapy. (A-B) Blood was collected from breast cancer patients at baseline, and 24 hours after the first cycle of paclitaxel therapy (n=15). The percentage of TMPs (expressing both MUC-1 and CD44) was evaluated by flow cytometry in baseline and post chemotherapy platelet-poor plasma samples. Fold-increase of TMPs (MUC-1+/CD44+) was calculated relative to baseline levels, and found to be statistically significant ($p<0.05$) using non-parametrical Wilcoxon signed-rank test (A). Representative dotplots of the flow cytometry analysis are shown (B). *, $p<0.05$; ***, $p<0.001$.

Figure 1

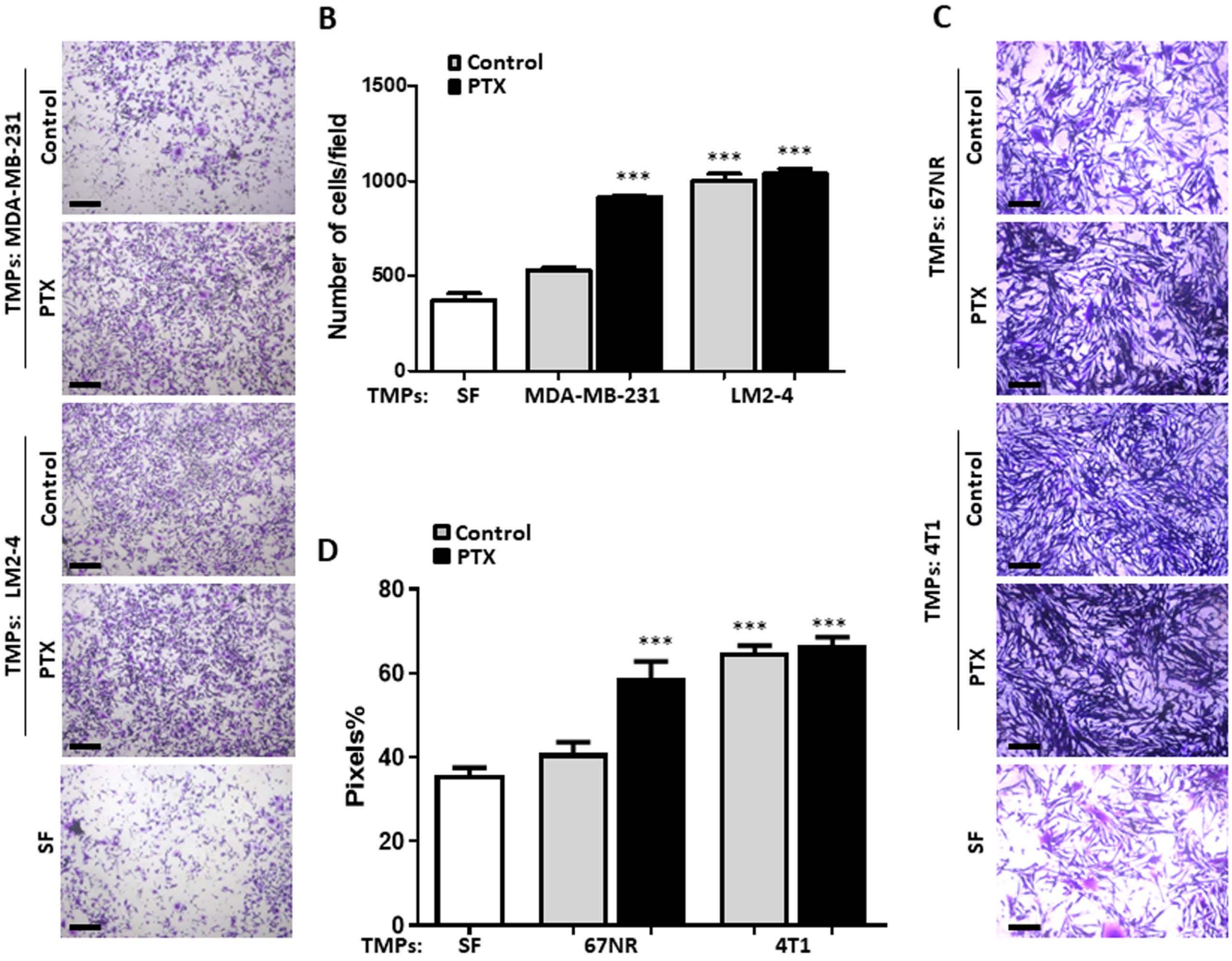
A
TMPs: MDA-MB-231
Control
PTX
TMPs: LM2-4
Control
PTX
SF
B
Control
PTX
Number of cells/field
1500
1000
500
0
***
***
***
TMPs: SF MDA-MB-231 LM2-4
C
TMPs: 67NR
Control
PTX
TMPs: 4T1
Control
PTX
SF
D
Control
PTX
Pixels%
80
60
40
20
0
***
***
***
TMPs: SF 67NR 4T1

Figure 2

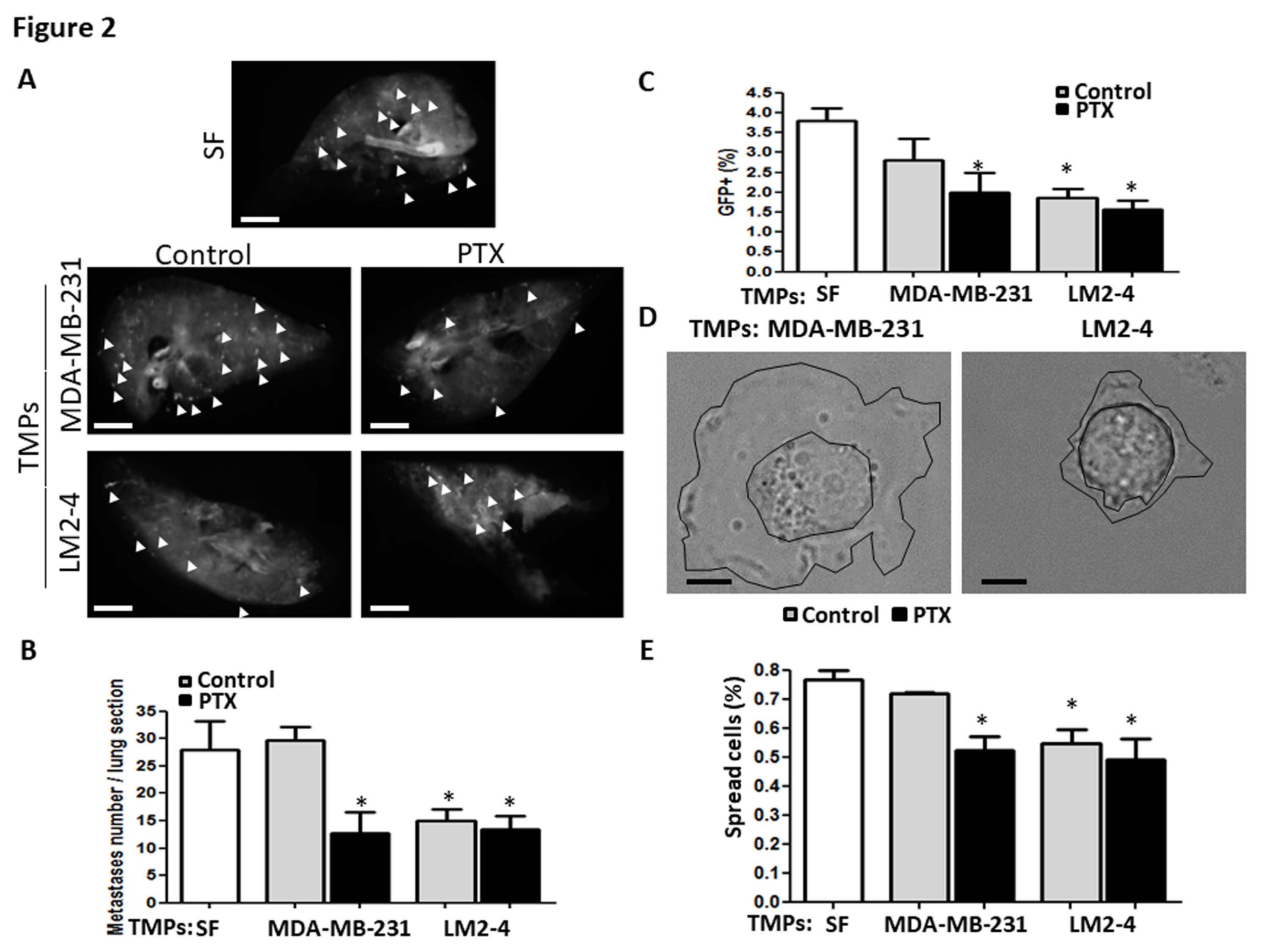
A
SF
Control
PTX
TMPs
MDA-MB-231
LM2-4
B
Control
PTX
Metastases number / lung section
TMPs: SF
MDA-MB-231
LM2-4
C
Control
PTX
GFP+ (%)
TMPs: SF
MDA-MB-231
LM2-4
D
TMPs: MDA-MB-231
LM2-4
Control
PTX
E
Spread cells (%)
TMPs: SF
MDA-MB-231
LM2-4

Figure 3

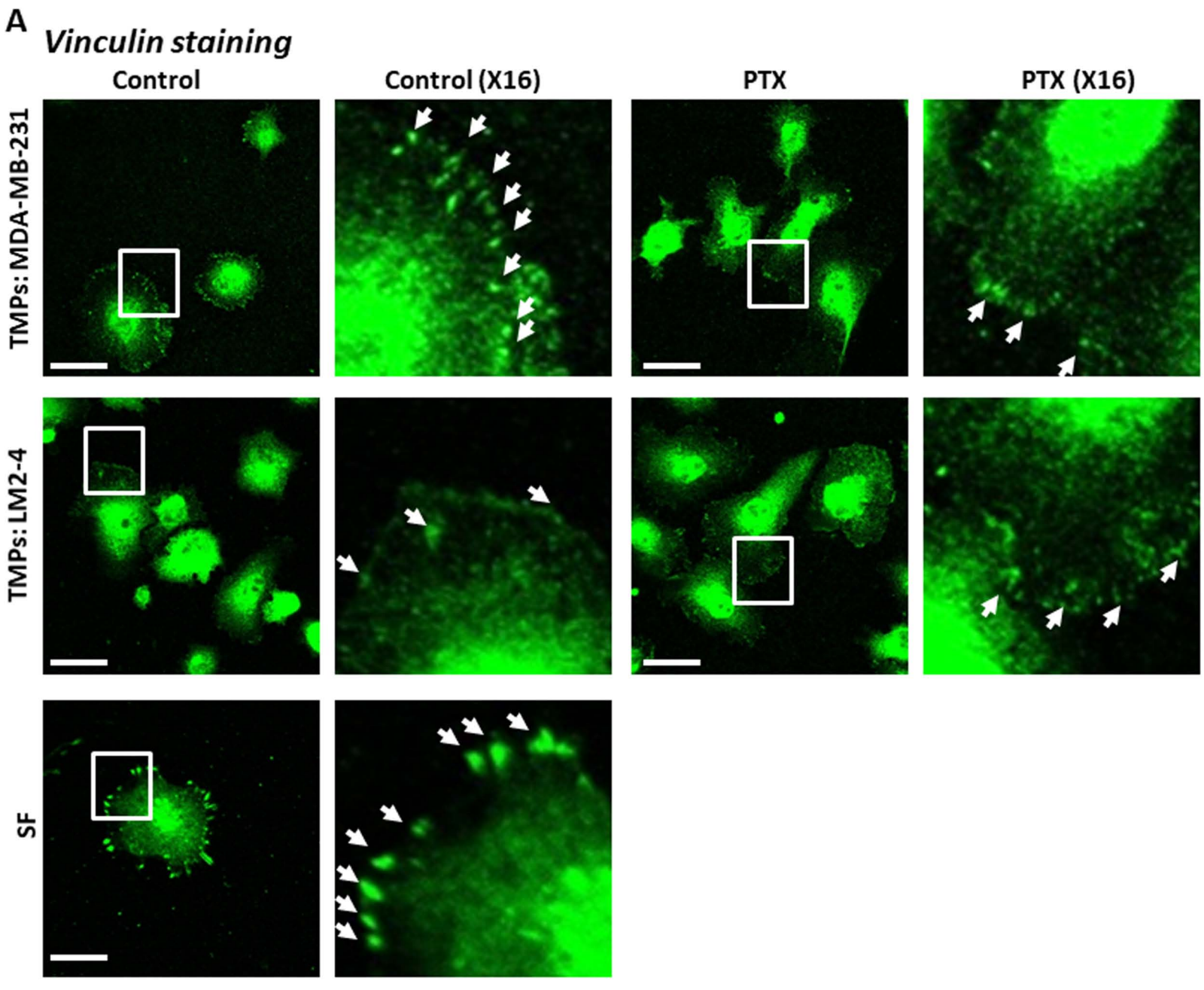
A
Vinculin staining
Control
Control (X16)
PTX
PTX (X16)
TMPs: MDA-MB-231
TMPs: LM2-4
SF

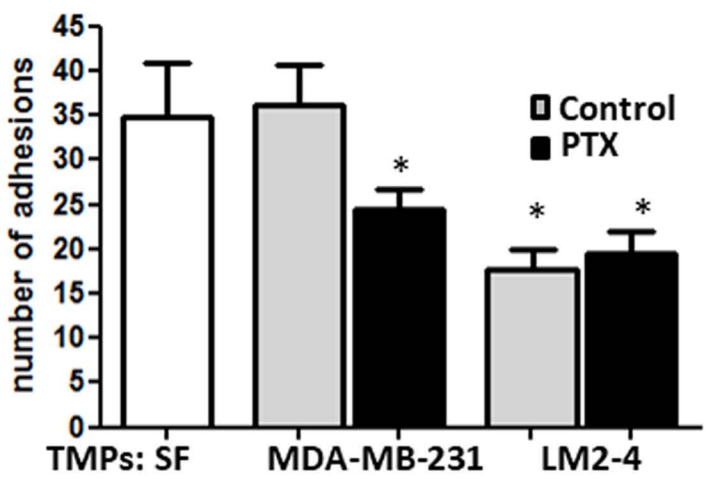
B
number of adhesions
Control
PTX
TMPs: SF
MDA-MB-231
LM2-4

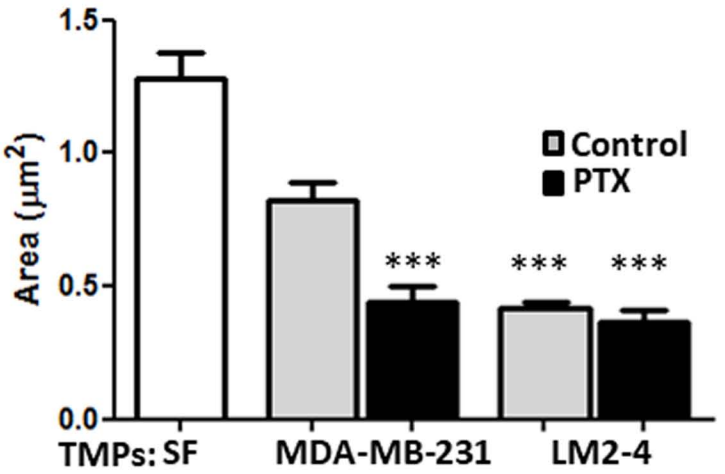
C
Area (μm²)
Control
PTX
TMPs: SF
MDA-MB-231
LM2-4

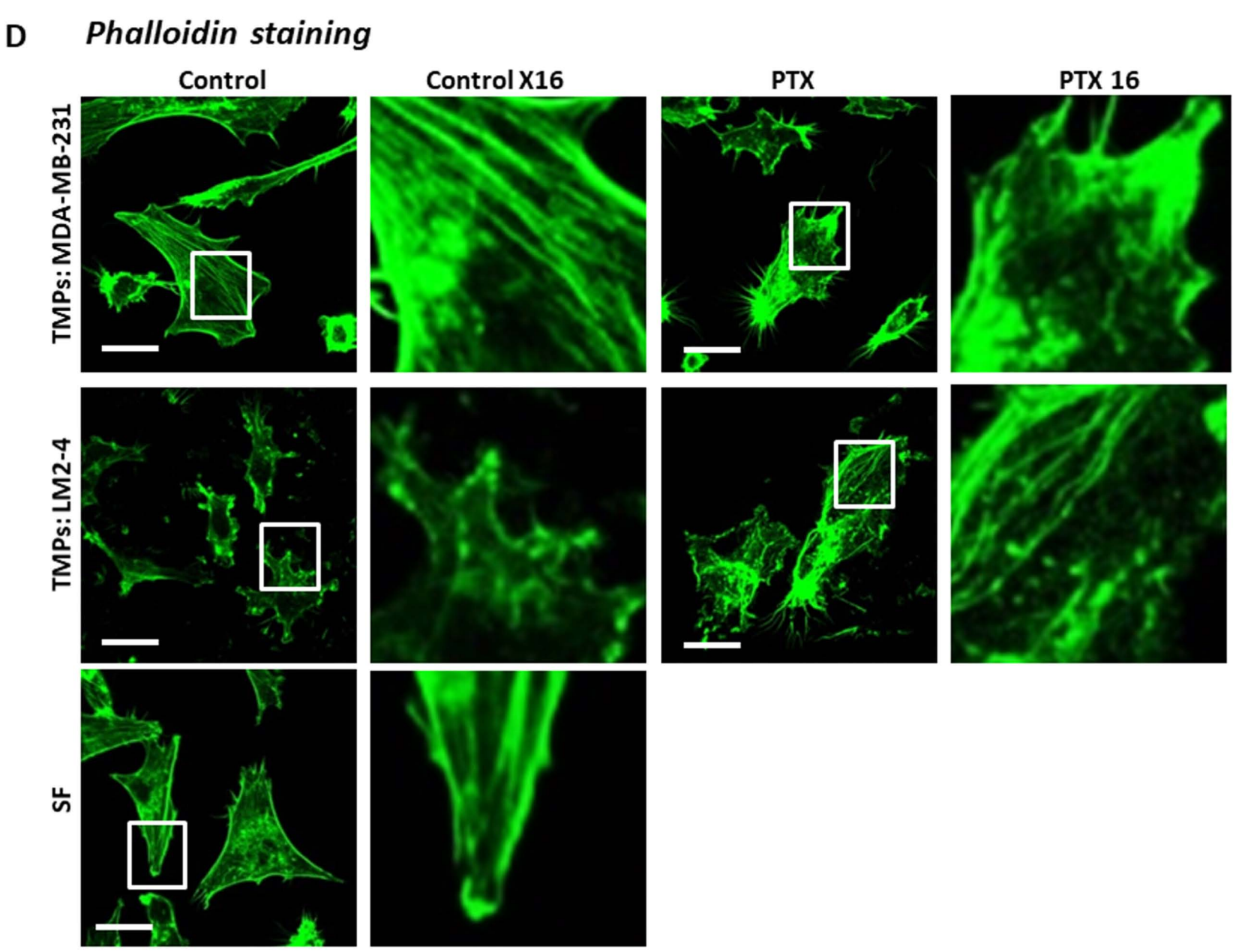
D
Phalloidin staining
Control
Control X16
PTX
PTX 16
TMPs: MDA-MB-231
TMPs: LM2-4
SF

Figure 4

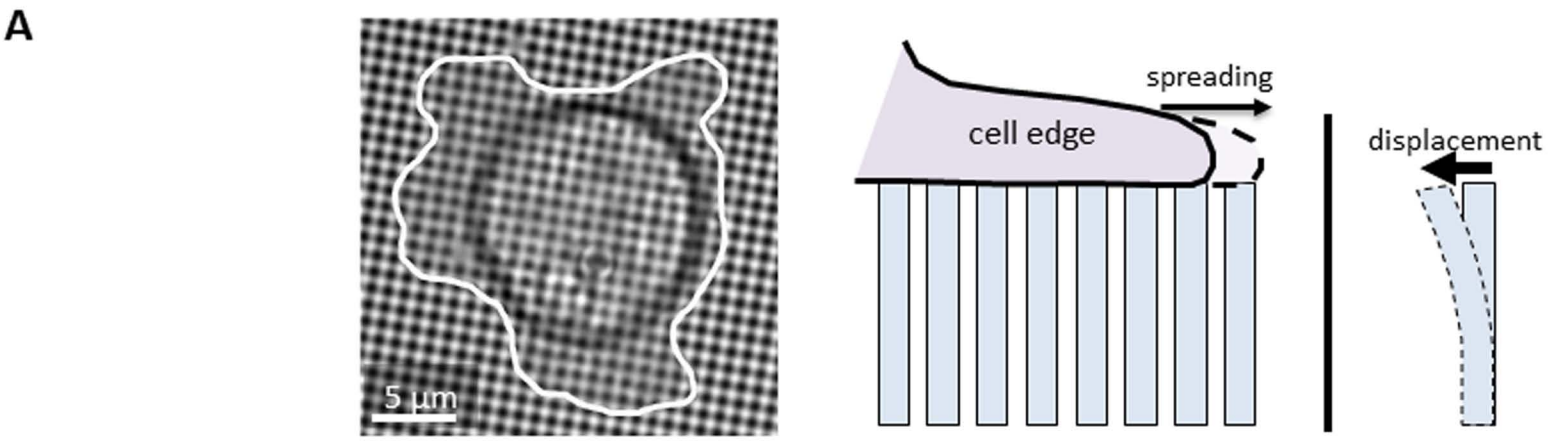
A
5 µm
spreading
cell edge
displacement
B
tEVs:
SF
MDA-MB-231-control
MDA-MB-231-PTX
LM2-4 control
LM2-4 PTX
Displacement (nm)
Time (s)
5 nm
5 s
C
tEVs:
MDA-MB-231
MDA-MB-231-Cont
MDA-MB-231-PTX
LM2-4-Cont
LM2-4-PTX
Average no. of releases per sec
peak size (nm)
D
TMPs:MDA-231-MB
LM2-4
SF
Cont
PTX
Cont
PTX
P-Pax-
T-Pax-
GAPDH-
E
Control
PTX
P-Pax / T-Pax fold change
TMPs: SF
MDA-MB-231
LM2-4

Figure 5

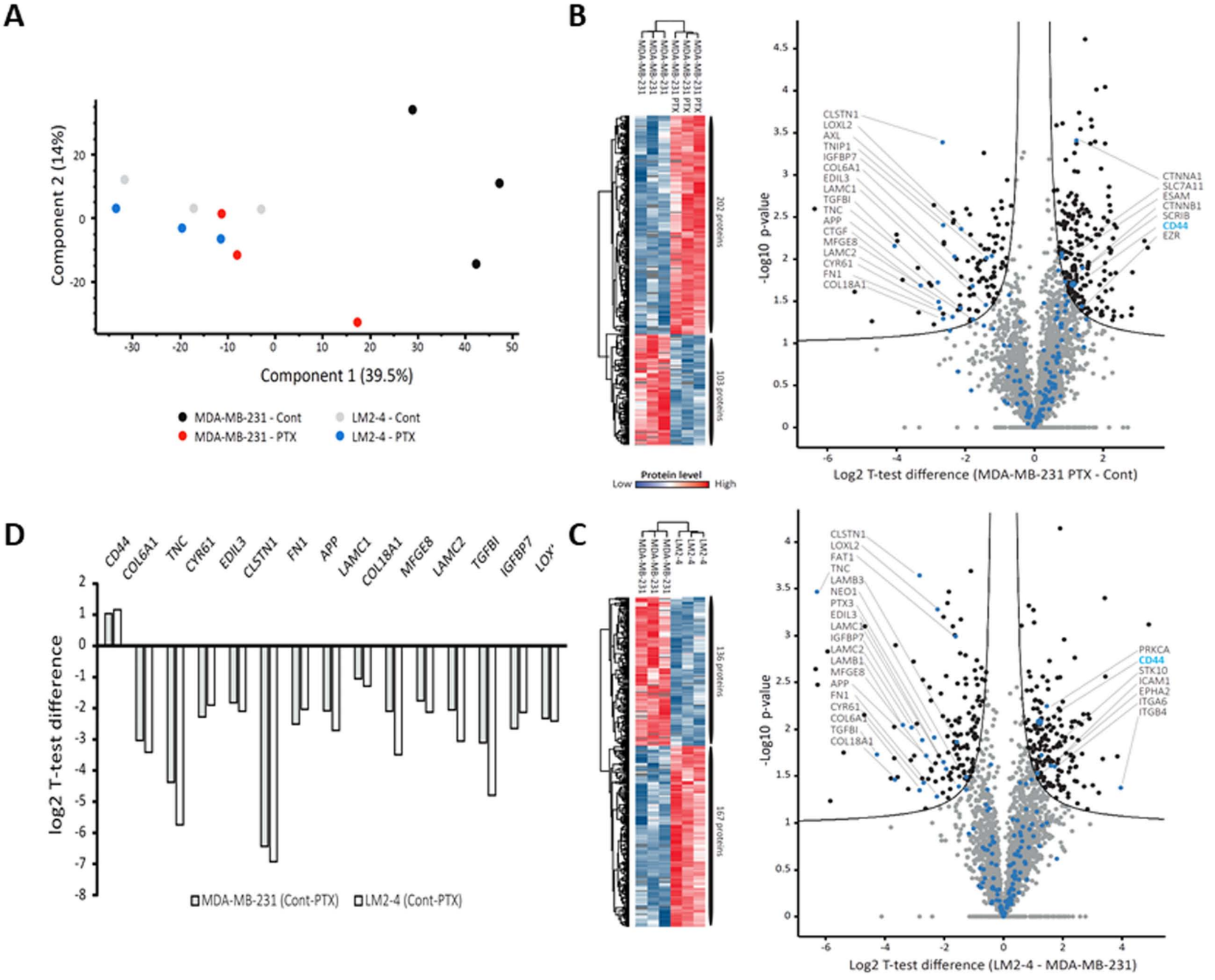
A
Component 2 (14%)
Component 1 (39.5%)
MDA-MB-231 - Cont
MDA-MB-231 - PTX
LM2-4 - Cont
LM2-4 - PTX
B
202 proteins
103 proteins
Protein level
Low
High
-Log10 p-value
Log2 T-test difference (MDA-MB-231 PTX - Cont)
CLSTN1
LOXL2
AXL
TNIP1
IGFBP7
COL6A1
EDIL3
LAMC1
TGFBI
TNC
APP
CTGF
MFGE8
LAMC2
CYR61
FN1
COL18A1
CTNNA1
SLC7A11
ESAM
CTNNB1
SCRIB
CD44
EZR
D
log2 T-test difference
MDA-MB-231 (Cont-PTX)
LM2-4 (Cont-PTX)
C
136 proteins
167 proteins
-Log10 p-value
Log2 T-test difference (LM2-4 - MDA-MB-231)
CLSTN1
LOXL2
FAT1
TNC
LAMB3
NEO1
PTX3
EDIL3
LAMC1
IGFBP7
LAMC2
LAMB1
MFGE8
APP
FN1
CYR61
COL6A1
TGFBI
COL18A1
PRKCA
CD44
STK10
ICAM1
EPHA2
ITGA6
ITGB4
E
CD44 expression
Control
PTX
Log2 LFQ intensity
MDA-MB-231
LM2-4

Figure 6

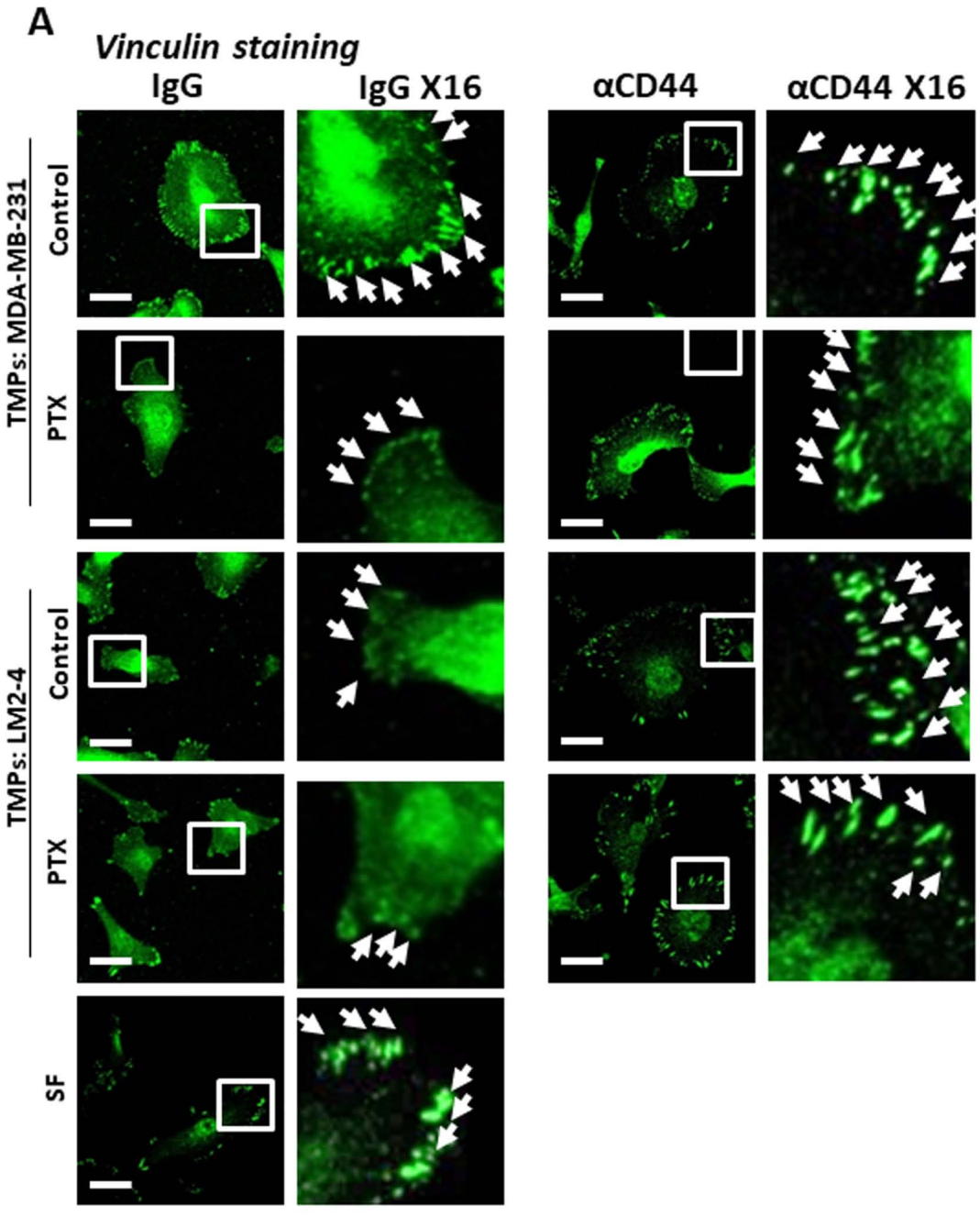
A
Vinculin staining
IgG
IgG X16
αCD44
αCD44 X16
TMPs: MDA-MB-231
Control
PTX
TMPs: LM2-4
Control
PTX
SF

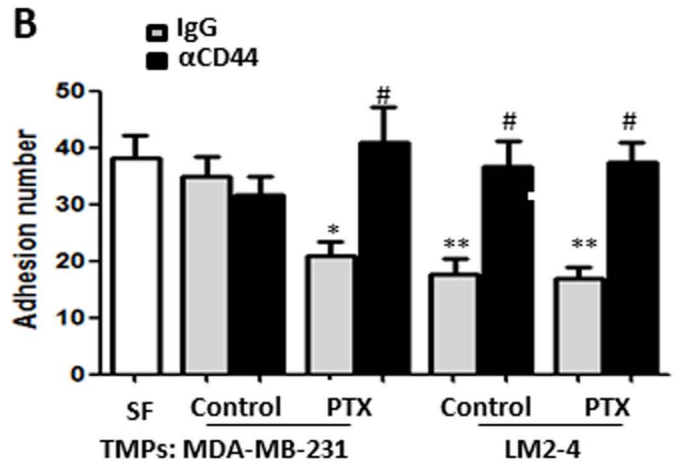
B
IgG
αCD44
Adhesion number
SF
Control
PTX
Control
PTX
TMPs: MDA-MB-231
LM2-4

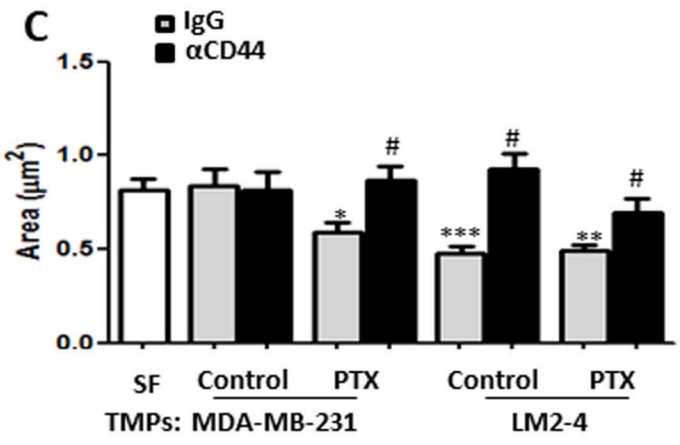
C
IgG
αCD44
Area (μm²)
SF
Control
PTX
Control
PTX
TMPs: MDA-MB-231
LM2-4

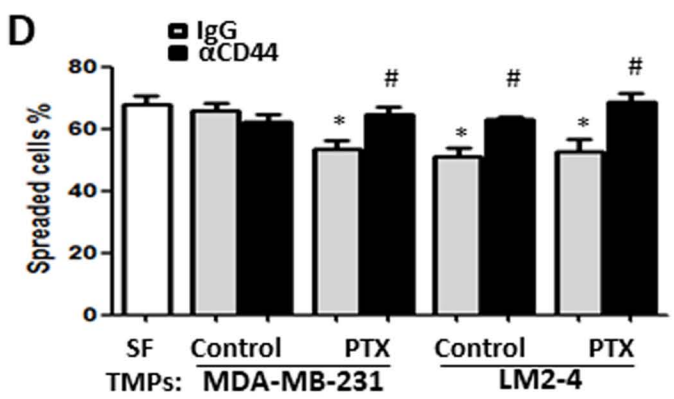
D
IgG
αCD44
Spreaded cells %
SF
Control
PTX
Control
PTX
TMPs:
MDA-MB-231
LM2-4

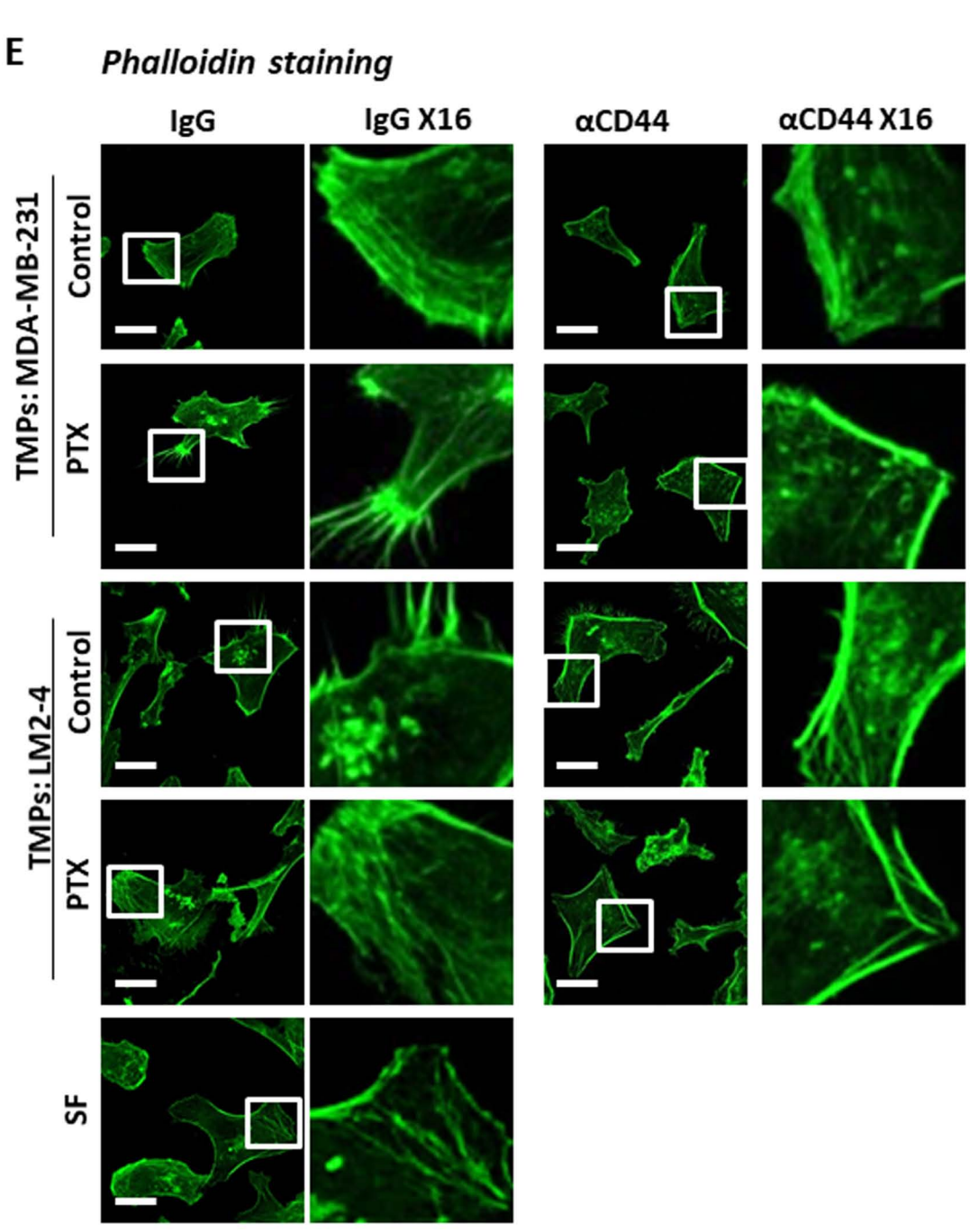
E
Phalloidin staining
IgG
IgG X16
αCD44
αCD44 X16
TMPs: MDA-MB-231
Control
PTX
TMPs: LM2-4
Control
PTX
SF

Figure 7

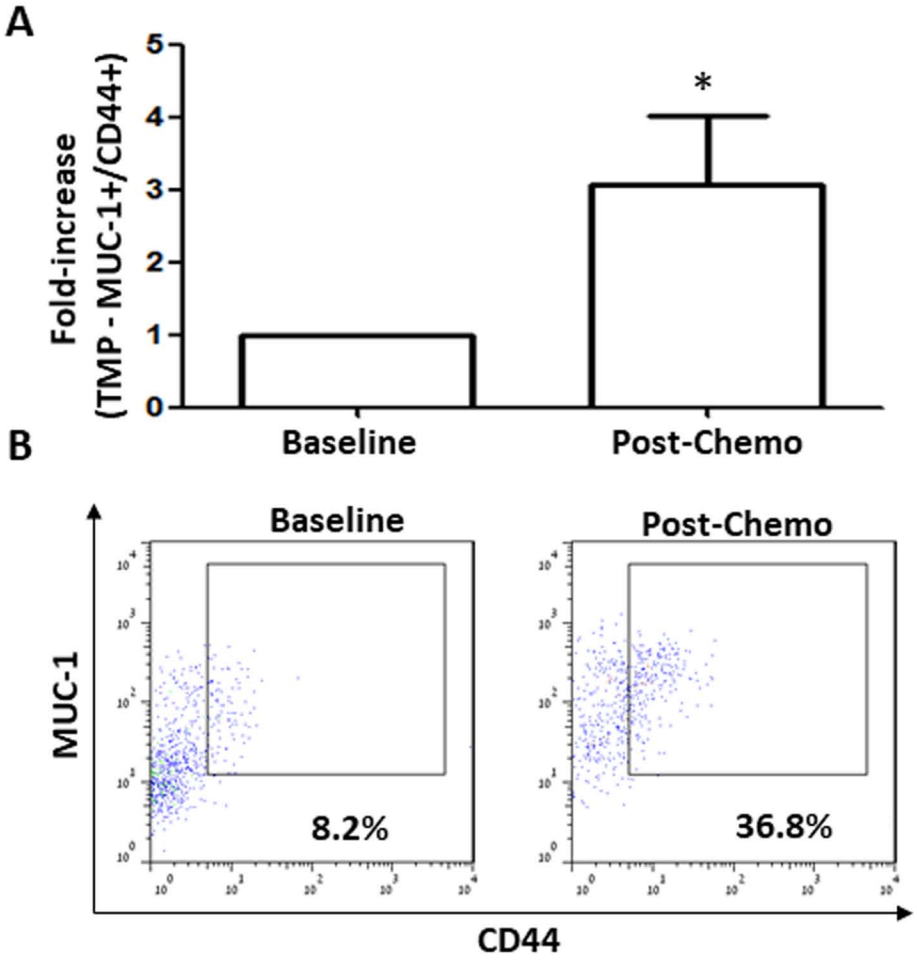
A
Fold-increase
(TMP - MUC-1+/CD44+)
5
4
3
2
1
0
*
Baseline
Post-Chemo
B
Baseline
Post-Chemo
MUC-1
8.2%
36.8%
CD44